Turbulent channel flow tests

June 5, 2018

Channel Flow tests

The idea for this investigation is to check the cause for non-existant eddy viscosity in the channel for the $Re_\tau = 395$. We would perform two set of simulations on the mesh resolution 192x64x96 (Mesh1). We would write out all the quantities i.e. gradients $\frac{\partial v_i}{\partial x_i}$, strain rates contraction and the traceless tensor formulated with the square of the velocity gradient tensor. In short, it would be same as we did previously in the poiseuille flow simulations and the Taylor green vortex simulations.

List of Figures

List of Tables

Contents

1   Introduction

The idea for this investigation is to check the cause for non-existant eddy viscosity in the channel for the $Re_\tau = 395$. We would perform two set of simulations on the mesh resolution 192x64x96 (Mesh1). We would write out all the quantities i.e. gradients $\frac{\partial v_i}{\partial x_i}$, strain rates contraction and the traceless tensor formulated with the square of the velocity gradient tensor. In short, it would be same as we did previously in the poiseuille flow simulations and the Taylor green vortex simulations.

i. Mesh 1 AA2016Wale. We will perform the simulation for total 300,000 time steps and write out the data only for the $300,000^{th}$ time-step. In this tests we will not perform any kind of averaging, but write out all the details as discussed above. The idea here is to observe the order for the different quantities written out and to estimate the orgin of the error.

ii. Mesh 1 AA2016Wale - smaller perturbation number (ϵ). Here we will perform the same simulation as above, but with the smaller ϵ added to make the system well-poised. The definition of which is as follows:

$$\nu_t = (C_w \Delta)^2 \, \frac{\left(S_{ij}^d S_{ij}^d\right)^{3/2}}{\left(\bar{S_{ij}}\bar{S_{ij}}\right)^{5/2} + \left(S_{ij}^d S_{ij}^d\right)^{5/4} + \epsilon} \tag{1}$$

where, ϵ in our case is of the order $\sim 10^{-8}$.

In this simulation we will change the value of ϵ to $\sim 10^{-30}$ or lower as the order of the terms in the numerator and the denominator are in between $\sim 10^{-18}$ to $\sim 10^{-25}$. Adding the epsilon of $\sim 10^{-8}$ in the denominator, which is relatively a larger number, is the reason we do not see the eddy viscosity in the channel. The purpose of this test is to see if we get the same orders of magnitude of the eddy viscosity as obtained in the tests performed using Matlab.

1.1   Discussion 9th May

I. Test 1. Here we have to improve the conditioning for the eddy viscosity in a more general way, rather than adding a constant approximately. The idea as discussed by professor is as follows:

$$\begin{aligned}
A^{3/2} &= \left(S_{ij}^d S_{ij}^d\right)^{3/2}, \\
A^{5/4} &= \left(S_{ij}^d S_{ij}^d\right)^{5/4}, \\
B^{5/2} &= \left(\bar{S_{ij}}\bar{S_{ij}}\right)^{5/2}
\end{aligned} \tag{2}$$

When terms of the equation 2 are replaced in the equation for 1 it looks as

follows (not considering ϵ now):

$$\nu_t = (C_w\Delta)^2 \frac{A^{3/2}}{B^{5/2} + A^{5/4}},$$

$$OP = \frac{A^{3/2}}{B^{5/2} + A^{5/4}} \tag{3}$$

Now in the equation 3 let's divide by $A^{5/4}$ and OP would like:

$$OP = \frac{A^{3/2}A^{-5/4}}{\left(B^{5/2}/A^{5/4}\right) + 1} \tag{4}$$

Some sort of this modification can give a general conditioning of the eddy viscosity.

II. Channel flow. Pressure and the density are negative i.e. mass deficit in the channel

III. Taylor green vortex. Finer resolution with changed value of ϵ.

$$OP = \frac{A^{1/4}}{\left(B^{1/2}/\left(A^{1/4} + 10^{-10}\right)\right)^5 + 1} \tag{5}$$

1.2   Next steps $15^{th} May$

Since the reason for the missing eddy viscosity is found, $\epsilon = 10^{-30}$, and an appropriate wale model co-efficient, $C_W = 0.55$, we should start the wale model simulations on the channel flow.

i. AA2016Wale and OneWale
ii. AA2016wale with double precision. This will be a comparison to see if any significant changes are present in the flow.

2 Lattice Boltzmann theories

3 Turbulence theories

4 Implementation

5 Model set-up and theories

Apart from the free shear flows, most turbulent flows are bounded by one or more solid surfaces depending on whether they belong to class of the internal or external flow of fluids i.e. flow through pipes and flow over a car respectively. In this investigation one of the simplest internal flow has been chosen for the validation & testing of the implementation: fully developed channel flow. In this flow the mean velocity vector will be parallel to the wall and this flow is considered to be of prime importance as it has played a prominent role in the development of the study of the wall bounded turbulent flows [3]. [3] has described the fundamental theories of the full developed channel flow in great detail along with the reasoning of certain behaviour of the fluid near the channel wall. [4] also has a good compilation on the fully developed channel flow. In general it serves as a very good reference for the beginners in LES.

In this section an attempt will be made to address the main challenges faced in the LES simulations that will include the mesh statistics, initialization, experimental settings, boundary conditions, LB solver specifics followed by post-processing and the final discussions of the results.

5.1 Turbulent channel flow

Fully developed turbulent channel flow is a classic benchmark case and has been studied extensively to investigate and understand the mechanics of wall-bounded turbulent flows. It is the geometrical simplicity of this case that has lured to a large number of, computational (DNS) and experimental, investigations being carried out for the turbulent channel flow over the years and as a result, an adequate database (DNS data) for certain Re-numbers is already available. [5](MKM, Moin & Jiminez) Link too. Historical progression in the turbulent channel flow simulations have been very well documented in the literature by Kim et al. Also, Kim has pointed out several difficulties related to the experimental measurements and how numerical simulations serve as an essential tool, alongside the experimental results, for the study of the wall-bounded turbulence. The recent development along with the comparison of the DNS results of the turbulent channel flow simulations for higher Re-numbers is documented in [Moser] As shown in the figure a three dimensional flow through a rectangular duct is considered and the aspect ratio of the duct is $\gg$ than 1. The dimensions of the 3d box are shown in the table 1

$Nominal Re_\tau$	L_x x L_y x L_z
395	6δ x 2δ x 3δ

Table 1: The size of the domain in x, y, z directions

The size of the 3D duct has been chosen in accordance with the reference literature of [6].

5.1.1 Governing equations

Turbulent channel flow is fully developed, where the velocity statistics along the stream-wise direction remain constant i.e. $\partial U/\partial x = 0$, and statistically one dimensional, where the flow statistics vary only in the wall-normal(y) direction.

Since the flow is two-dimensional, there is no mean flow in the span-wise direction i.e $W = 0$ and thus the gradient of the span-wise velocity in the span-wise direction is zero i.e. $\partial W/\partial z = 0$. The mean continuity equation for the incompressible flow results in the mean wall normal velocity gradient to be zero:

$$\partial V/\partial y = 0 \tag{6}$$

The eq. 6 when integrated, within the wall limits [0,2δ], gives $V = const(y)$ and using the no-slip boundary condition, $U_i = 0$, applied at the walls results in $V = 0$. Now to satisfy the resulting continuity equation eq. 6, V has to be zero everywhere in the domain. Using the above made considerations and applying it to the mean stream-wise momentum equation we will have the following force balance:

$$\frac{\partial \tau}{\partial y} = \frac{\partial P}{\partial x} \tag{7}$$

where $\tau = \left(\mu \frac{\partial U}{\partial y} - \rho \overline{u_i u_j} \right)$ is the total shear stress.

The eq. 7 shows that the total shear stress gradient and the pressure gradient balance each other in the full developed channel flow. It shows an equality of the form $f(x) = g(y)$ and for this equality to hold it is important that both $f(x)$ and $g(y)$ are individually constants. In eq. 7 both the gradients are dependent on different variables and thus they must be individually constants for this equality to hold.

$$\frac{\partial P}{\partial x} = const \ \& \ \frac{\partial \tau}{\partial y} = const$$

Total shear stress is the summation of the viscous stress, $\mu \frac{\partial U}{\partial y}$, and the Reynolds stress, $-\rho \overline{u_i u_j}$. At the wall with the no-slip boundary condition applied, the Reynolds stresses are reduced to zero and thus the shear stress near the wall or to be specific at the wall would entirely be dominated by the viscous stresses. Shear stress can be defined here as the *wall shear stress*, the region where the viscous stresses are dominant:

wall shear stress

$$\tau_w = \mu \frac{\partial U}{\partial y} \tag{8}$$
$$\tau(0) = \tau_w = -\tau(2\delta)$$

Now we can integrate the eq. 7, from 0 to 2δ, for the pressure gradient and express the solution in terms of the τ_w:

$$-\frac{\partial P}{\partial x} = \frac{\tau_w}{\delta} \ , \tag{9}$$

From the fully developed channel flow it is known that the mean velocity profile (time-averaged) remains constant. It is clear from eq. 8 that wall shear stress is linearly proportional to the velocity gradient near the wall. A constant velocity profile implies that the wall shear stress will also be constant in a fully developed channel flow. Thus from eq.9 we can say that the pressure gradients is constant. $\tau(y)$ is anti-symmetric about the mid channel height $\tau(\delta)$ and thus the total

shear stress is zero there. Integrating the eq. 7, from 0 to some y, with the no-slip boundary condition at the wall results in the following solution:

$$\tau\left(y\right) = \tau_w \left(1 - \frac{y}{\delta}\right) \tag{10}$$

The pressure gradient in eq. 9 is negative as the viscous effects decreases the pressure along the stream-wise direction. It is this pressure gradient that drives the flow through the infinite parallel plates. For a given pressure gradient and the half-channel height we get a linear shear stress profile from eq. 9 and 10 independent of the fluid properties and the state of the fluid motion (laminar or turbulent) [3]. Also, several investigations have showed that the total shear stress profile is anti-symmetric about the channel mid height $y = \delta$ and thus $\tau\left(\delta\right) = 0$.

5.1.2 Scaling units

The Reynolds stresses decreases towards the wall, remain zero at the wall and so does the eddy viscosity (*Boussinesq hypothesis*). The value of the eddy viscosity ranges from zero, at the wall, to several orders of magnitude higher than the molecular viscosity, in the core region of the turbulent boundary layer [1]. From the figure. 1 it can be seen that the velocity profile changes more slowly (more flatter compared to the parabolic flow profile) in the core of the turbulent boundary layer, where the eddy viscosity is higher than the molecular viscosity, and there is an abrupt change in the velocity profile near the wall, where the molecular viscosity is dominant. The turbulent flow profile has the largest gradient near the wall.
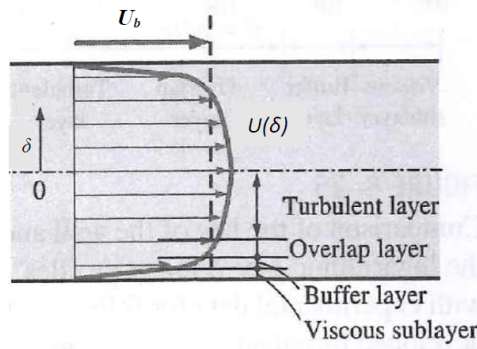

Figure 1: Velocity profile in the fully developed channel flow [1]

Turbulent flow along the wall can be considered to consist of four different layers, characterised by their distance from the wall. All four layers have been approximately shown in figure 1. The layer closet to the wall is the viscous sub-layer, where the viscous effects are dominant. The velocity profile changes linearly with the distance from the wall and the flow is streamlined. Next to the viscous sub-layer is the buffer layer, where the turbulent stresses start to develop, but still the viscous stresses are dominant. Above the buffer layer is the overlap layer, where the turbulent stresses are significant, but still not dominant

enough as the viscous stresses. The layer above the overlap layer for the rest of the flow is the outer or turbulent layer, where the turbulence stresses dominate over the viscous stresses.

A single analytical relation for the entire turbulent velocity profile is not suitable, as different regions or layers execute different flow characteristics. The best possible option is to find the key parameters or the functional forms using the dimensional analysis and later on experimental data can be used to obtain the numerical values of the any constants.

i. Viscous sub-layer : With the no-slip boundary condition applied at the wall, $u_i(0, t) = 0$, the entire contribution to the shear stress is purely via viscous stresses i.e. τ_w. From eq. 8 it is clear that shear stress is proportional to the molecular viscosity. The thickness of this layer is very small, but it plays an important role on the flow characteristic because of the presence of large velocity gradients in it. The velocity profile remains linear in this layer and also it has been shown in certain experiments [1]. Since the velocity profile is linear the gradient in the equation 8 remains constant i.e. $\partial U/\partial y = U/y$. Thus the wall shear stress can be written as:

$$\frac{\tau_w}{\rho} = \frac{\nu U}{y} \tag{11}$$

Near the wall the important parameters are : τ_w, ρ, ν. The square root of the term on the left hand side has the dimensions of velocity and thus we define a new parameter as the **friction velocity**, u_τ:

$$u_\tau = \sqrt{\frac{\tau_w}{\rho}} \tag{12}$$

Replacing u_τ in the eq. 11 we have **the law of wall**:

$$\frac{U}{u_\tau} = \frac{u_\tau y}{\nu} \tag{13}$$

The quantity ν/u_τ has the dimensions of length and it is called **viscous length**, δ_ν, and it is used to nondimensionalze the distance from the wall, y. In the analysis of the boundary layer flow, it is convenient to work with the nondimensionalised distance and the velocity. The nondimensionalised quantities are represented with a +.

Nondimensionalised variables :

$$y^+ = \frac{yu_\tau}{\nu} \ and \ u^+ = \frac{U}{u_\tau} \tag{14}$$

Normalised law of the wall :

$$u^+ = y^+ \tag{15}$$

This law shows a very good correlation with the experimental data for smooth surfaces for $0 \leq u_\tau y/\rho \leq 5$. Thus for the $y^+ = 5$ we will have the linear velocity
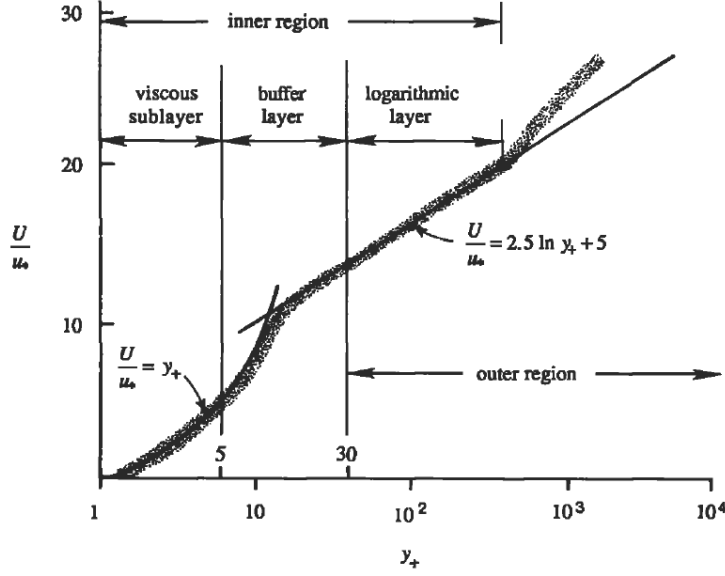
Figure 2: Nondimensional velocity u^+ vs. the nondimensional distance y^+ (plotted in logarithmic scale) [2]

profile and the viscous sub-layer.

ii. Overlap layer: From the dimensional analysis and the experimental results it proved that the velocity in the overlap region is proportional to the logarithm of distance and it can be expressed as:

$$u^+ = \frac{1}{\kappa} \; ln \; y^+ + \; B \; or \; u^+ = 2.5 \; ln \; y^+ + \; 5.0 \tag{16}$$

where κ and B are constants and equal to 0.40 and 5.0 respectively. The eq. 16 is called the *logarithmic law* and the overlap layer is also called as the *logarithmic layer* or *log-law layer*. It is clear from the figure 2 that the eq. 16 represents the experimental data quite satisfactorily from $y^+ \geq 30$ till outer region. Neither eq. 16 nor the eq. 13 represents the experimental data satisfactorily in the buffer layer. From Figure. 2 it is seen that :

viscous sub-layer : $y^+ \leq 5$

buffer layer : $y^+ \geq 5$ till $y^+ \leq 30$

logarithmic layer : $y^+ \geq 30$ till $y^+ \leq 10^3$

iii. Outer layer: The velocity law for this region is:

$$\frac{(U_{max} - U)}{u_\tau} = \frac{1}{\kappa} \; ln \; \left(\frac{y}{\delta}\right) \tag{17}$$

The difference between the mean center line velocity, U_{max}, and the mean velocity, U is called the **velocity defect** and thus this law is called the **velocity**

defect-law. In this region the turbulent stresses are dominant compared to the viscous stresses and this is also seen from the eq. 17: the normalised velocity profile in the core region of the turbulent channel flow is dependent on the half-channel height and is not dependent on the viscosity.

5.2 Reynolds number

Since the Reynolds number is used to characterize the flow, great care was taken to simulate the same flows i.e. same Reynolds number as that of the DNS data was used. The dimensionless Reynolds number requires three parameters for its definition: characteristics length (δ), characteristic velocity (V_{ch}) and the kinematic viscosity (ν) of the fluid.

$$Re = \frac{V_{ch}\delta}{\nu}$$

Several choices of V_{ch} are possible, but in this investigation two different V_{ch} have been chosen and the respective Reynolds number are as follows :

i. Friction Reynolds number (Re_τ):

$$Re_\tau = \frac{u_\tau\delta}{\nu} = \frac{\delta}{\delta_\nu} \tag{18}$$

ii. Bulk Reynolds number (Re_b):

$$Re_b = \frac{U_b\,2\delta}{\nu} \tag{19}$$

5.3 Computational Domain and Meshing

We are interested to investigate the fully developed turbulent channel and that implies a sufficient length and width of the domain for the flow in the channel to be fully developed. Since the stream-wise and the span-wise directions are homogeneous the periodic boundary conditions is used at either side of the two homogeneous directions. This implies that we have a flow between two infinite parallel planes, Figure 3. Since the artificial periodic boundaries are enforced great care has to be taken that the domain is long enough to avoid this artificial boundary conditions from influencing the results.*Moin et.al* [7] has specified certain aspects to be considered in the process of choosing the dimensions of the flow domain for the numerical simulation of the turbulent channel flow. According to [7] the experimental two-point correlation functions have to be considered for choosing the stream-wise (L_x) and the span-wise (L_z) lengths. The usage of periodic boundary conditions is justified if the length of the side of the computational domain is at least twice the distance, at which the correlation function becomes zero.

To validate the LES results of the fully developed turbulent channel flow the DNS data from the database of [6] for the $Re_\tau = 395$ is used. The authors have shown the adequacy of the domain by performing the two-point spatial correlations and the same domain size has been chosen for the performing the LES of channel flow, Table 1. Thus, no separate study for two-point correlation has been performed in this investigation.
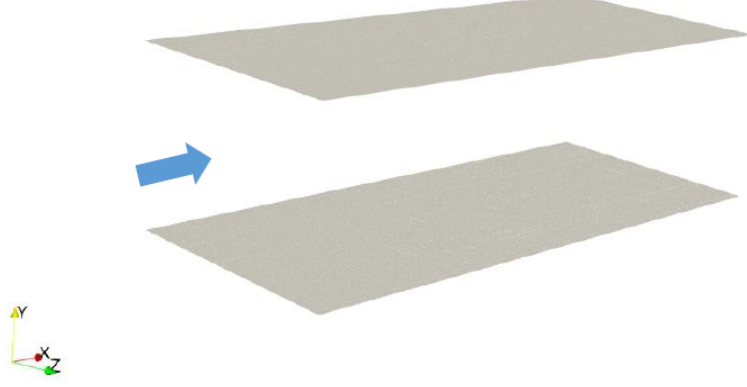
Figure 3: Flow between the infinite parallel plates

$NominalRe_\tau$	L_x x L_y x L_z
395	6δ x 2δ x 3δ

Table 2: The size of the domain in x, y, z directions

5.4 Initial conditions

It is known from the theory of the internal fluid flow that there exists a hydro-dynamic entry length (L_h), starting from the inlet (x = 0), that the fluid has to travel, in the channel, for the flow to become fully developed. This means when we integrate the flow governing equations, in time, the fluid has to travel the distance L_h $(\tilde{x} = 10H)$ in every time-step, to generate a fully developed flow, which is unnecessary considering the computational efforts and also the storage requirements. The idea is to consider only that portion of the channel which will be fully developed, turbulent and not the initial part (L_h) of the channel. This implies we will have to provide specific initial conditions for the flow to become fully developed and turbulent.

Different approaches have been used by different authors to generate the initial condition for the incompressible, three-dimensional, unsteady, turbulent channel flow simulations.*Moin et.al* [7] has specified few consistency criteria for initial velocity field. *Sagaut* [8] & *Fröhlich* [4] have a concide description of most commonly used approaches with their respective advantage, disadvantages and their applications to suitable flows. Few of the several approaches mentioned in [8] & [4] will be discussed here.

i. First approach: In this approach a simulation is performed for some Reynolds number smaller than the one to be simulated. The resulting fields of this simulations are then used as the starting point for the required Reynolds number and is simulated further in time until a steady state, where the statistics of the flow do not change with time, is achieved. This approach is termed as *Precursor simulation* in several literature.

ii. Second approach: In this approach a laminar flow is chosen as the base flow and certain set of disturbances are applied on the base flow. The base

flow super-imposed with disturbances is then integrated in time until the flow transitions to a turbulent flow. This approach is computationally intensive, as the flow takes time to become turbulent. There are several options available to impose the disturbances on to the base flow. Several authors have used this approach for the generating appropriate initial conditions. In this investigation this approach has been used.

For the initialisation of our simulations the work of *Eugene de Villiers* [9] is closely followed. *Eugene de Villiers* introduced some sort of near wall streak cycle, where he uses the fundamentals of the turbulent structures near the walls. A parabolic flow profile is chosen as the base flow. To generate the parabolic flow profile the bulk mean velocity, $U_b = 0.1335 \ m/s$, which was computed by [9], from the mean velocity DNS data of [6] for $Re_\tau = 395$, is used.

Parabolic flow profile has been applied in the stream-wise direction, $u(y, 0)$, on all the fluid nodes in the domain. Figure 4 shows the parabolic profile used as the base flow. A combination of sine and cosine waves have been used to break the flow symmetry and to develop the turbulence in the flow.
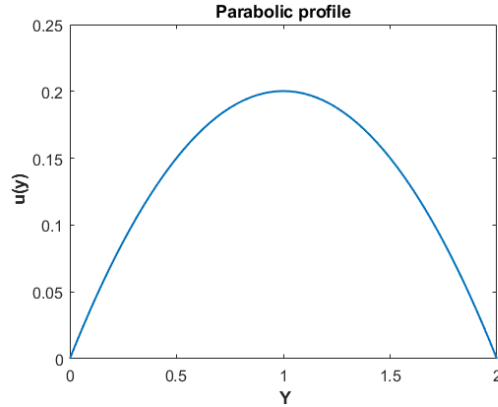

Figure 4: Parabolic flow profile with $U_b = 0.1335 \ m/s$

Initially the the disturbances were applied on to the parabolic profile, but that approach was quite time consuming. It took approximately 4.5 million time-steps for the flow to be turbulent. Next approach was to apply the disturbances in the wall-normal direction, v. This approach reduced the time it took for the flow to be turbulent, 100,000 time-steps. The exact equations for the initialisations have been specified in the the Appendix.

A   Initial conditions

$$u = \mu \frac{\partial U}{\partial y}$$
$$v = \tau_w = -\tau \left(2\delta\right) \qquad\qquad (20)$$
$$w = 0$$

References

[1] Y.A. Cengel and J.M. Cimbala. *Fluid Mechanics: Fundamentals and Applications.* McGraw-Hill, New Delhi, 2 edition, 2011.

[2] P.K. Kundu and I.M. Cohen. *Fluid Mechanics.* Academic Press, 525 B Streek Suite 1900, San Diego, California 92101-4495, USA, 2002.

[3] S.B. Pope. *Turbulent Flow.* Cambridge University Press, Cambridge, UK, 2001.

[4] Jochen Fröhlich. *Large Eddy Simulationen turbulenter Strömungen.* Teubner/GWV Fachverlage GmbH, Wiesbaden, DE, 2006.

[5] http://turbulence.ices.utexas.edu/.

[6] R.D. Moser, J.D. Kim, and N.N. Mansour. Direct numerical simulation of turbulent channel flow up to $Re_\tau = 590$. *Physics of Fluids*, 11:943–945, 1999.

[7] W.C. Reynolds P.Moin and J.H.Ferziger. Large eddy simulation of incompressible turbulent channel flow. Technical report number t-12, Thermosciences Division, Department of Mechanical Engineering, Stanford University, Stanford, California, 1978.

[8] P. Sagaut. *Large Eddy Simulation for Incompressible Flow.* Springer Verlag, 2002.

[9] Eugene de Villiers. *The Potential of Large Eddy Simulation for the Modeling of Wall Bounded Flows.* PhD thesis, Thermofluids Section, Department of Mechanical Engineering, Imperial College of Science, Technology and Medicine, Kensington, London SW7 2AZ, 2006.